High rectification in organic diodes based on liquid crystalline phthalocyanines

Petru Apostol, Juliana Eccher, Marta Elisa Rosso Dotto, Cassiano Batesttin Costa, Thiago Cazati, Elisabeth A. Hillard, Harald Bock, Ivan H. Bechtold

High rectification in organic diodes based on liquid crystalline phthalocyanines

Petru Apostol[a], Juliana Eccher*[b], Marta Elisa Rosso Dotto[b], Cassiano Batesttin Costa[c], Thiago Cazati[c], Elizabeth A. Hillard[a], Harald Bock[a] and Ivan H. Bechtold*[b]

[a]Centre de Recherche Paul Pascal, Université de Bordeaux & CNRS, 115 Avenue Schweitzer, 33600 Pessac, France.
[b]Departamento de Física, Universidade Federal de Santa Catarina−UFSC, 88040-900 Florianópolis, SC, Brazil.
[c]Departamento de Física, Universidade Federal de Ouro Preto – UFOP, 35400-000, Ouro Preto, MG, Brazil.

The optical and electrical properties of mesogenic metal-free and metalated phthalocyanines (PCs) with a moderately sized and regioregular alkyl periphery were investigated. In solution, the individualized molecules show fluorescence lifetimes of 4-6 ns in THF. When deposited as solid thin films the materials exhibit significantly shorter fluorescence lifetimes with a bi-exponential decay (1.4-1.8 ns; 0.2-0.4 ns) that testify to the formation of aggregates via π-π intermolecular interactions. In diode structures, their pronounced columnar order outbalances unfavorable planar alignment and leads to excellent rectification behavior. Field-dependent charge carrier mobilities are obtained from the *J-V* curves in the trap-limited space-charge-limited current regime and demonstrate that the metalated PCs display an improved electrical response with respect to the metal-free homologue. The excited-state lifetime characterization suggest that the π–π intermolecular interactions are stronger for the metal-free PC, confirming that the metallic centre plays an important role for the charge transport inside these materials.

1 Introduction

Phthalocyanines (PCs) have found widespread use as charge transport materials in organic electronics research due to their good chemical stability and their large flat π-electron system that allows good π-orbital contact between neighboring molecules.[1-4] Metal PCs have been used as dyes or pigments for various different applications, they are very promising materials for modern optoelectronic devices due to high chemical and thermal stability.[5] Whilst unsubstituted PCs are insoluble in common organic solvents, four- or eightfold alkyl or alkoxy substitution leads to highly soluble PCs that can be solution-processed.[6] The nature of the ligand substituent and of the metal ion in the core of the ligand influences strongly the PCs properties. In polar solvents a large red shift of the Q absorption band has been observed.[7] The addition of large solubilizing substituents might worsen the charge transport properties

due to the dilution of the electronically active molecular cores by a large amount of electronically inert alkyl groups, but the introduction of suitably shaped flexible substituents might also lead to improved intermolecular π-electron contacts via the formation of columns of closely stacked aromatic disks surrounded by a nanosegregated alkyl periphery in a columnar liquid crystal (LC) or plastic crystal state.[8,9]

Such organized macroscopic structures merit special attention due to the self organizing characteristics that allow to modify and to control the optoelectronic properties.[10-12] One of the main advantages of liquid crystalline PCs in relation to the other discotic macrocycles is their strong absorption in the visible and NIR regions.[13] Columnar LC PCs have been promising candidates for photovoltaic applications[14,15] and a columnar LC CuPC was efficiently applied as an organic active layer in thin film transistors, where the device performance was shown to strongly depend on the annealing procedure.[16]

We have recently reported that racemic 3-(2-butyloctyloxy)phthalonitrile can be tetramerized to a regiosymmetrically tetrasubstituted PC and its transition metal(II) complexes, where the four branched alkoxy substituents lead to the formation of columnar mesophases with moderate phase transition temperatures.[17] Here we present the electronic behavior in solution-processed organic diodes of the metal-free (H_2-) and metalated (Cu- and Ni-) tetraalkoxy-PCs in order to correlate the optoelectronic properties with the molecular organization and film structure.

2 Experimental

X-ray diffraction (XRD) experiments were performed with an X'Pert PRO (PANalytical) diffractometer using CuKα beam (λ = 1.5405Å) and using the X'Celerator detector to collect the diffracted radiation. Films were prepared by depositing an amount of powder on a glass plate, where the temperature was controlled with a TCU2000-Temperature Control Unit (Anton Paar). The diffractograms were collected in continuous mode (2 to 30 degrees) at room temperature after cooling from the isotropic phase.

Cyclic Voltammetry (CV) was performed in a three electrode cell, utilizing an Autolab PGStat20 potentiostat, driven by GPES software (General Purpose Electrochemical System, Version 4.4, EcoChemie B.V., Utrecht, the Netherlands), a platinum wire counter electrode, a 1.6 mm platinum disc working electrode, and a non-aqueous reference electrode comprised of a silver wire in a 0.01 M solution of $AgNO_3$ and 0.1 M tetrabutylammonium perchlorate in acetonitrile; the analytes (approximately 1 mM) were dissolved in DCM supplemented with

0.1 M tetrabutylammonium hexafluorophosphate and degassed by bubbling argon prior to measurement.

A SpectroVision UV-vis spectrophotometer, model DB-1880S, was used to record the absorption spectra of the PCs in solution and spin-coated films, whereas, for the emission measurements, a Hitachi fluorescence spectrophotometer, model F-7000, was used, with the samples excited at a wavelength of 636 nm. Time-resolved fluorescence decays were recorded using the technique of time-correlated single photon counting[18] with a FluoTime 200 (PicoQuant). Excitation was provided using a pulsed diode laser (instrument response function around 100 ps, 20 MHz repetition rate) at a wavelength of 636 nm. Fluorescence was collected perpendicular to excitation and passed through a polarizer set at the magic angle. The detection system consisted of a monochromator and a MCP-PMT photomultiplier (Hamamatsu R3809U-50). FluoFit Software was used to analyze the decay curves and the plots of weighted residuals and reduced chi-square ($\chi 2$) were used to accurate the quality of the fittings during the analysis procedure. The measurements were done on tetrahydrofuran (THF) solutions at a concentration of 12 mg/mL and spin-coated films produced by solutions of 30 mg/mL in THF with 2000 rpm during 30 seconds.

Optical textures of the films were obtained from an Olympus BX50 polarizing optical microscope (POM) in transmission mode, equipped with a Mettler Toledo FP-82 hot stage to control the temperature. The images were recorded with a CCD camera coupled to the optical microscope. The thickness and roughness of the spin-coated films was probed with an atomic force microscope (AFM), using a Nanosurf EasyScan2 apparatus in tapping mode with a scanning rate of 1.0 Hz covering a size of 20 μm × 20 μm with (512 × 512) pixels.

For the electrical characterization of phthalocyanines **1-3**, diodes were fabricated by solution processing of the compounds in THF at a concentration of 30 mg/mL. Indium tin-oxide (ITO) coated glass plates with a sheet resistance of about 15 Ω/□ were used as conductive substrates. A thin layer of poly(3,4-ethylenedioxythiophene):poly(styrenesulfonate) (PEDOT:PSS) was deposited by spin-coating on cleaned substrates at 3000 rpm during 30 seconds, followed by annealing at 110 °C for 5 minutes. The active organic layers were spin-coated at 3000 rpm for 30 seconds. Top electrodes were obtained by vacuum deposition (10^{-7} mbar) of Al (80 nm) at a deposition rate of 1 Å/s. The active area of the diodes was 10 mm^2. The *J*/*V* curves were measured in ambient conditions and at room temperature (25 ^{o}C) using a Keithley's Series 2400 Source Measure Unit (SMU) Instruments.

3 Results and discussion

We investigated three PCs: Metal-free **1**, copper derivative **2** and nickel homolog **3**, (Fig. 1). As reported previously, all three exhibit a plastic crystalline columnar mesophase of rectangular symmetry at room temperature that forms upon cooling (**1**: below 40°C, **2**: below 70°C, **3**: below 45°C) from a higher-temperature LC mesophase of hexagonal (**1**) or rectangular (**2**, **3**) symmetry, the transition enthalpies between the liquid crystalline and plastic crystalline states being barely noticeable by calorimetry.[17] **1** and **3** can be obtained in a conventional crystalline state (with a strong melting enthalpy to the LC state of *ca.* 40 kJ/mol in both cases) by slow crystallization from a bad solvent, whereas in the case of **2**, the plastic crystalline state is directly obtained by slow precipitation from solution. Fig. 2 shows the XRD patterns of solid films of compounds **1-3**, measured at room temperature after cooling from the isotropic state. Inset of Fig. 2 displays the low angle region, where the peaks could be identically indexed as in the powder XRD experiments presented previously, where a detailed discussion about the molecular organization is presented.[17] Despite the fact that all the three compounds present a rectangular tilted columnar plastic crystalline phase at room temperature, compound **1** is the only one to show a hexagonal mesophase upon cooling from the isotropic liquid, indicating that delocalized π–π intermolecular interactions are more pronounced in **1**, whereas tilt-inducing metal-nitrogen interactions play a dominant role for the intermolecular interactions in **2** and **3**. In all three cases, it is to be presumed that spin-coating leads to the same plastic crystalline state at room temperature that is observed after cooling down the pure material from elevated temperatures.

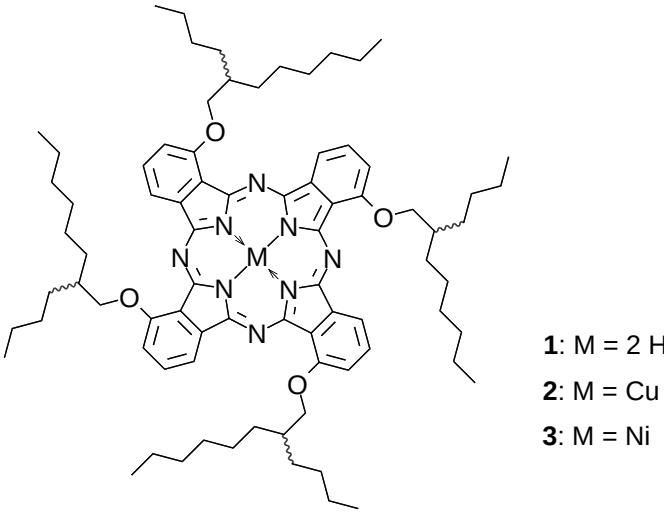

Fig. 1 Chemical structure of the investigated PCs **1-3**.

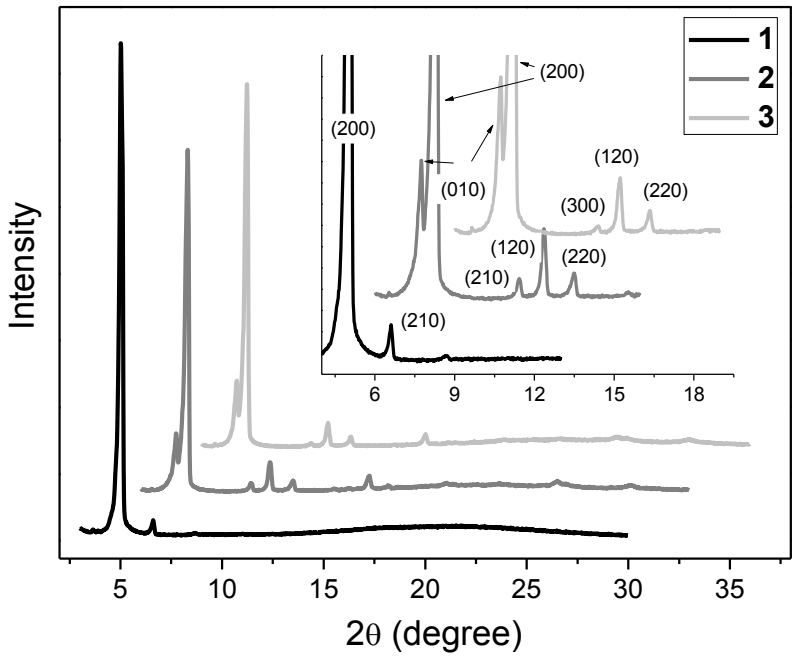

Fig. 2 XRD spectra of PCs **1**-**3** in solid films measured at room temperature after cooling from the isotropic phase. Inset, low angle region with Miller indices.

The electrochemical behavior of **1**-**3** is characterized by three quasi-reversible oxidation waves and two reversible reduction waves in the cyclic voltammograms between −2.2 and 1.4 V vs. Fc/Fc^+ (CVs, Fig. 3). The potential of the first oxidation wave depends on the presence of a metal; it is found at significantly lower potential (*ca.* 0.021 V) for the metal-containing compounds than for the free ligand (0.098 V). The second oxidation wave is less sensitive with potentials of 0.292 (±0.006), 0.287 (±0.003) and 0.280 (±0.001) V for **1**, **2** and **3**, respectively. A third, larger peak, occurs at potentials between 0.854 (±0.003) and 0.765 (±0.005) V.

Differences between the free ligand and metal-containing compounds are more marked in the reduction chemistry, with a significant shift to more negative potentials for the coordination compounds. Two reversible waves are observed at −1.339 (±0.001) and −1.734 (±0.006) V for the free ligand, while **2** and **3** are very similar, with potentials of −1.446 (±0.003) and −1.855 (±0.01) V and −1.457 (±0.003) and −1.895 (±0.01) V, respectively.

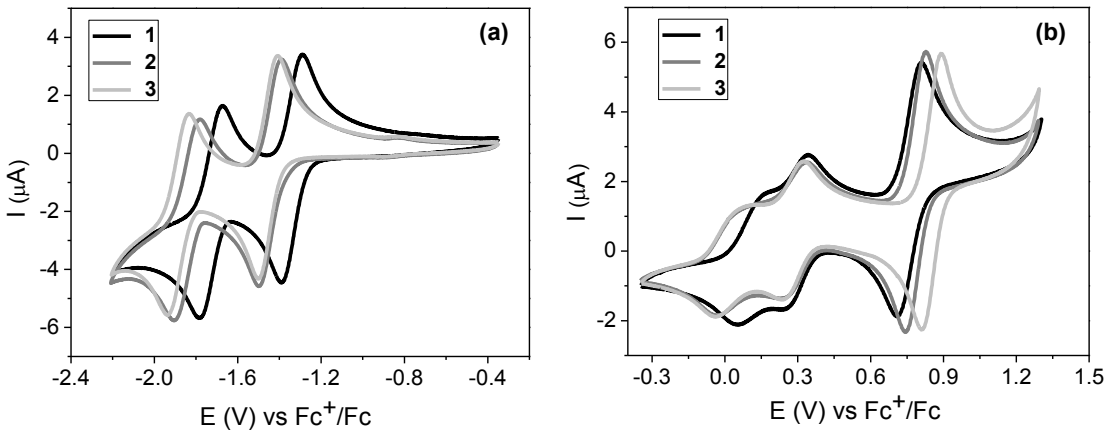

Fig. 3 Cyclic voltammograms of **1-3** in CH_2Cl_2 supplemented with 0.1 M Bu_4NPF_6. 1.6 mm Pt working electrode: (a) reduction processes and (b) oxidation processes. Current intensities were normalized for concentration using the factor 1.15 for **1** and 1.06 for **3**.

The qualitative similarity of the CVs for **1-3** is consistent with the previous observation that the first reduction and first oxidation in Ni, Cu and metal-free phthalocyanines occur on the ligand.[19] From the first oxidation and reduction potentials and with ferrocene/ferrocenium at −4.80 eV with respect to vacuum, HOMO and LUMO energies of E_{HOMO} (**1**) = −4.90 eV, E_{LUMO} (**1**) = −3.46 eV, E_{HOMO} (**2**) = −4.82 eV, E_{LUMO} (**2**) = −3.35 eV, E_{HOMO} (**3**) = −4.82 eV and E_{LUMO} (**3**) = −3.34 eV are obtained. These values are approximately 0.2 eV closer to vacuum than those of unsubstituted PCs,[20] illustrating the moderately electron-donating effect of the four *endo*-alkoxy substituents.

The absorbance spectrum of **1** (Fig. 4) is characteristic of phthalocyanines with two kinds of energy bands,[21] a so-called B (or Soret) band between 280-400 nm in the UV region and a Q band between 600-720 nm. The Q band is attributed to the π-π^* transitions from the HOMO to the LUMO. In the spin-coated thin film the Soret band is relatively more intense, whereas the Q band is broader and less defined than in solution, being associated to the aggregation of molecules via intermolecular interactions between the aromatic planes.[4] The vibronic structure clearly seen in the solution spectrum reflects the different coupling patterns in solution and solid state.[22]

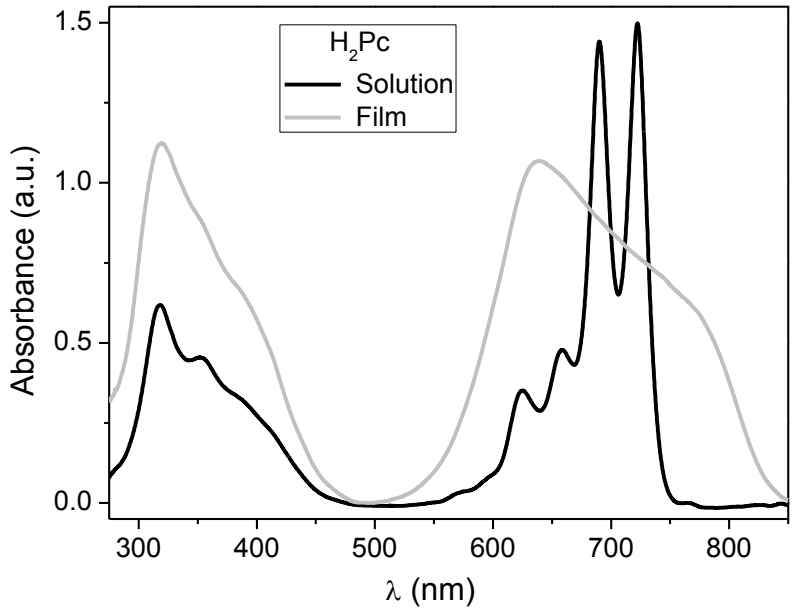

Fig. 4 UV-vis absorption spectra of **1** in THF and in film.

The band gap energies of the Q band were determined from the analysis of the absorption edges in solid films[23] and were estimated to be 1.48, 1.55 and 1.57 eV for **1**, **2** and **3**, respectively. These values agree within ±0.1 eV with the electrochemical band gaps determined by CV, 1.44 eV (**1**), 1.47 eV (**2**) and 1.48 eV (**3**). The absorption spectra of PCs **2** and **3** in THF and in film were similar to PC **1** and can be seen at the Supporting Information, Fig. S1.

The singlet excited-state lifetimes of **1**-**3** in THF solvent and spin-coated thin films were investigated by time-resolved fluorescence spectroscopy. The lifetimes of the PCs in solution and spin-coated films are shown in Table 1. The PCs **1**-**3** in solution exhibited mono-exponential decays with a singlet excited-state lifetime in the nanoseconds range. The lifetimes found for all PCs in THF are similar to long-lived excited states observed for monomeric PCs in solution.[24,25] Bi-exponential decays are usually observed for aggregated PC species in solution where their lifetimes are characterized by intermediate and fast fluorescence lifetimes, and where the fastest component becomes dominant upon increasing the concentration.[26]

The fluorescence decays of the PCs **1**-**3** spin-coated films were bi-exponential showing two distinct excited-state lifetimes that are both shorter than the lifetimes observed in THF solution. Moreover, the relative amplitude of the second short-living exponential

component (A_2) becomes predominant over the first one (A_1), suggesting that the second might be due to co-planar π-stacking. The formation of aggregates due to π–π intermolecular interactions in solid thin films was also observed by Bertoncello and co-workers for sulfonated CuPc films deposited by a layer-by-layer technique.[27] At Fig. S2 of the Supporting Information it is possible to compare the mono-exponential fitting for PC **1** in solution with the bi-exponential fitting in spin-coated film.

The shorter excited state lifetimes in the condensed film, and especially, the fact that the second time is dominant, agrees with the evidence from the absorption measurements where a broader Q band is observed in the film. These effects indicate a strong aggregation of the molecules in the spin-coated films driven by π–π interactions. On comparing the film absorption spectra of the free-metal and the metalated PCs it is evident that the Q band broadening of the metal-free PC **1** is larger (see Fig. S1 at the Supporting Information). In addition, the highest A_2 value is also observed for **1**. Both results suggest that the π–π interactions are more pronounced for the free-metal PC. This can be explained by the fact that metal-nitrogen interactions between adjacent molecules may constrain the establishment of maximal π–π interactions in **2** and **3**.

Table 1 Emission wavelength maxima, lifetimes and relative amplitudes of **1-3** in THF solutions and spin-coated films after excitation at 636 nm.

	λ_{max}* /nm	τ_1 / ns	A_1 (%)	τ_2 / ps	A_2 (%)	χ^2
Solution in THF						
1	730.0	5.7 ± 0.1	100.0	-	-	1.019
2	728.0	4.1 ± 0.2	100.0	-	-	0,997
3	727.0	4.9 ± 0.1	100.0	-	-	0.978
Spin-coated film						
1	692.0	1.4 ± 0.3	10.3	281 ± 20	89.7	0.995
2	692.0	1.6 ± 0.7	16.1	320 ± 55	83.9	0.990
3	692.0	1.8 ± 0.2	27.6	359 ± 80	72.4	1.005

*Excited state lifetimes were measured at maxima of the emission intensities. The fluorescence spectra of **1-3** excited at 636 nm in solution and thin film are presented in Fig. S3 at the Supporting Information.

We found that rather smooth homogeneous PC layers of uniform thickness are obtained with thickness of 300 nm for **1-3**. AFM images obtained before and after annealing for PC **3** are shown in Fig. 5(a) and (b), respectively. The R_{rms} (Root Mean Square Roughness) of the film as-spun was 9.0 nm. After annealing, the R_{rms} value increased to 25.0 nm and the morphology of the film surface is quite different, where domains corresponding to birefringent textures typical of planar surface alignment are clearly seen (also observed by POM in Fig. 6). Fig. 5(b) also suggest partial dewetting, which can result in short-circuit after metallization. Films of metal-free **1** are somewhat less smooth in comparison with samples **2** and **3** before annealing. Before annealing the R_{rms} values for **1** and **2** are 17.5 nm and 7.4 nm, respectively. After annealing the R_{rms} for PC **2** increased to 18.4 nm. With metal-free **1**, annealing lead to large separated domains and feature sizes that exceeded the range of our AFM images. AFM images of **1** and **2** can be seen in Fig. S4 at the Supporting Information.

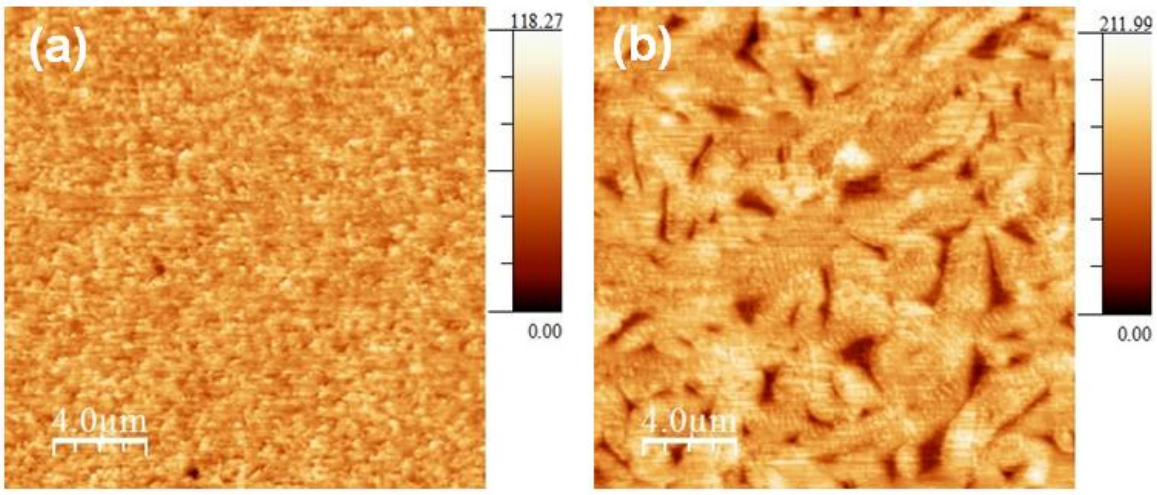

Fig. 5 AFM images of spin-coated film of **3**: as-spun (a) after annealing (b).

Unspecific textures consisting of small birefringent domains are observed by POM in the as-spun films (Fig. 6(a)), and annealing after fast cooling from the isotropic phase (**1**: 183°C, **2**: 268°C, **3**: 237°C) leads to birefringent textures typical of planar surface alignment (column axes parallel to substrate plane) (Fig. 6(b)). As such a planar surface orientation is unfavorable to good electrode-to-electrode charge transport in diodes (which in columnar LCs is found to be better within columns than from column to column,[28,29] and as indeed diodes made with annealed films tended to be short-circuited (probably due to partial dewetting during annealing,[30,31] we explored diodes with as-spun PC layers, whose birefringence also suggests predominantly planar alignment (in line with previous studies of unannealed open columnar LC films[32]), but which did not tend to short-circuits.

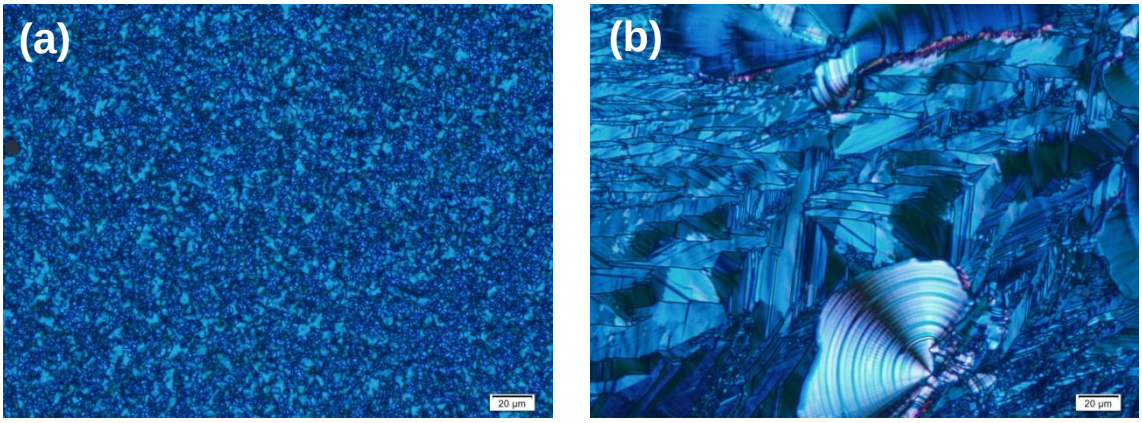

Fig. 6: POM textures of **3** as-spun film (a) and after fast cooling from the isotropic phase (b). The scale on the pictures is 20 µm.

To conform with well-established procedures,[33] we used poly(ethylenedioxythiophene): poly(styrenesulfonic acid) (PEDOT:PSS)-coated indium-tin-oxide (ITO) as glass-supported anode, onto which the PC layer was spun, and an aluminum cathode that was vacuum-deposited on top. The device structure used for electrical characterization of the PCs was ITO/PEDOT:PSS (80 nm)/PC **1**, **2** or **3** (300 nm)/Al (80 nm). The electrical measurements were performed at room temperature and under ambient conditions. The current density-voltage (*J-V*) characteristics are presented in Fig. 7. The energy levels of the PCs determined by cyclic voltammetry match well with the work functions of the PEDOT:PSS (~ 5.2 eV) and the Al electrode (~ 4.3 eV), leading a good charge carrier injection.

To our surprise, diodes made from any of the three homologs **1-3** show a degree of rectification higher than three orders of magnitude, see Fig. 6(a). These rectification ratios are much higher than those reported for a less regularly substituted PC, a hexagonal columnar liquid crystalline zinc PC derivative with a considerably larger electronically inert alkyl periphery,[21] giving rectification ratios of less than 10:1 in a very similar device configuration with ITO/PEDOT:PSS and Ca/Al electrodes. The strong rectification might result from close and regular molecular packing in the well ordered plastic rectangular columnar mesophases present in the materials **1-3**,[17] which provides intimate intermolecular π-orbital and metal-nitrogen interactions and therewith an efficient charge transport through the PC columns even in planar alignment, and thus leads to efficient charge evacuation after injection, avoiding the build-up of a counter-field that would outplay the built-in rectifier geometry. A rectification of 3 orders of magnitude was also obtained for a perylene-based columnar LC in a diode

structure in a similar edge-on configuration. Such effect results from a compact molecular packing induced to the organic film by thermal evaporation of the molecules.[34] Substrate-PC interactions were investigated by structural analysis in Chang-Hyun Kim et al.[35] They showed that in CuPC films deposited on ITO/PEDOT:PSS the molecules crystallized in an edge-on orientation whereas the deposition on graphene led to face-on orientation, providing higher rectification ratios. For CuPC films deposited in the device structure ITO/PEDOT:PSS/CuPC/Al, they obtained a ratio of rectification lower than 2 orders of magnitude. Mativetsky et al.[36] also used graphene to induce face-on stacking of CuPC thus improving the out-of-plane hole mobility.

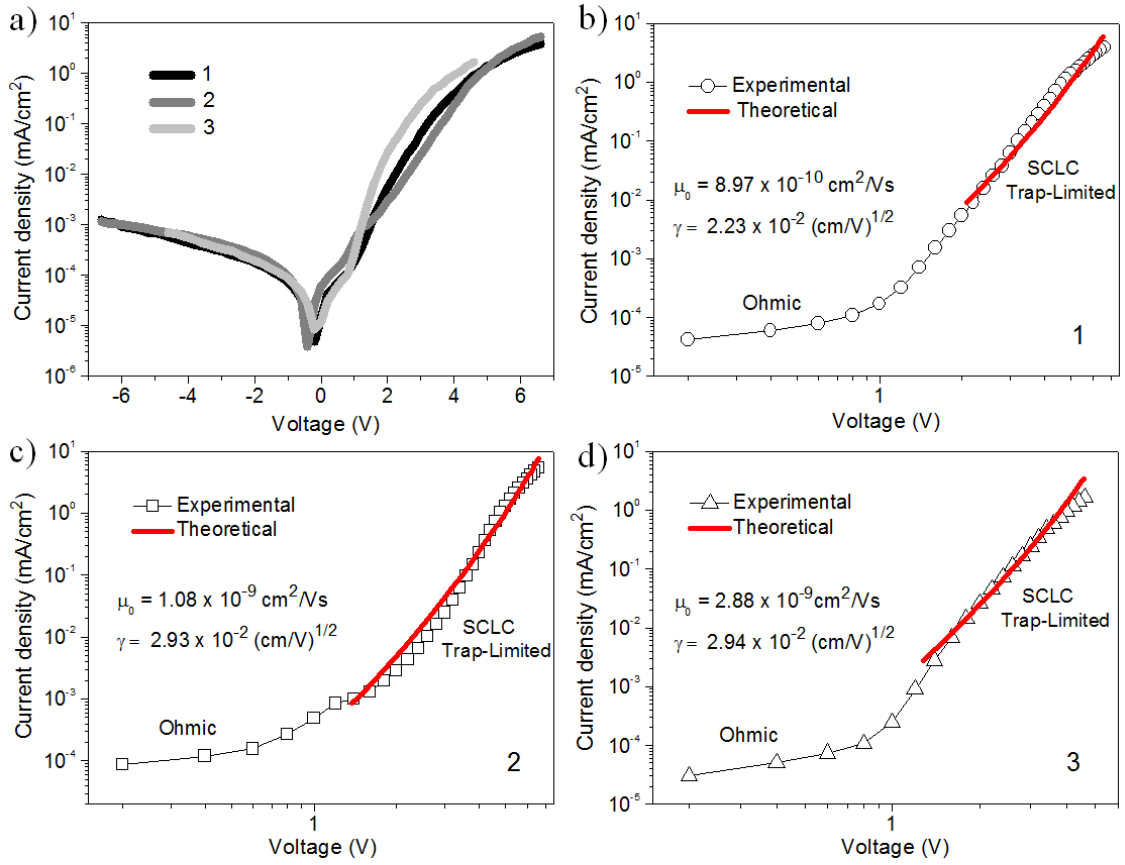

Fig. 7 Electrical characterization of the PC spin-coated films in the device configuration ITO – PEDOT:PSS (80nm) – PC (300nm) – Al (80nm). (a) Current density versus voltage. (b), (c) and (d) log-log plots of the J-V curves for compounds **1**, **2** and **3**. The red solid lines indicate the fitting at the trap-limited SCLC regimes.

The log-log plots of the current densities for **1-3** are presented in Fig. 7(b)-(d). The current densities follow an ohmic regime at low voltages and a trap-limited space-charge-limited current regime (SCLC, where the current from the injection of charge carriers from

the electrodes becomes dominant) at higher voltages. As the measurements do not obey the Mott-Gurney law ($J \propto V^2$), the charge mobilities were obtained directly from the *J-V* curves by fitting the trap-limited SCLC regimes with a theoretical model presented previously.[37] This model considers an electric field dependent mobility, given by $\mu(E) = \mu_0 e^{\gamma\sqrt{E}}$, where μ_0 is the carrier mobility at zero field and γ the field dependence of the mobility, with μ_0 and γ being the parameters extracted from the fitting. Values for μ_0 and γ were extracted for **1-3** and the respective fits are displayed as red solid lines in Fig. 7(b)-(d). The fits agree well with the experimental data obtained at the trap-limited SCLC regime. The μ_0 and γ values found for **1-3** are listed in Table 2, where the mobility values calculated from $\mu = \mu_0 e^{\gamma\sqrt{E}}$ are presented for an applied voltage of +4.6 V. The voltage dependence of the mobility is shown in Fig. S5 at the Supporting Information.

Table 2 Fitting values obtained for μ_0 and γ.

Parameter	**1**	**2**	**3**
μ_0 (cm^2/Vs)	8.97×10^{-10}	1.08×10^{-9}	2.88×10^{-9}
γ $(cm/V)^{1/2}$	2.23×10^{-2}	2.93×10^{-2}	2.94×10^{-2}
μ at applied +4.6 V (cm^2/Vs)	**1.28×10^{-5}**	**5.53×10^{-5}**	**2.46×10^{-4}**

At the same given voltage, mobility of **1** is the lowest and of **3** is highest. These mobilities of the order of 10^{-5} to 10^{-4} cm^2/Vs perpendicular to the column direction are low compared to the mobilities typically of 10^{-3} to 1.0 in the column direction reported for columnar liquid or plastic crystals, in agreement with the known anisotropy of mobility in columnar mesophases.[38-40] The higher Poole-Frenkel coefficients γ indicate that the hopping transport is easier for **3** and **2** than for **1**.

From the XRD patterns collected at room temperature cooling from the isotropic and the singlet excited-state lifetime measurements, where the exponential component (A_2) is higher, it is to be inferred that the free-metal PC **1** presents a higher contribution coming from the π–π intermolecular interactions, as is also corroborated by its broader absorption spectrum in the film compared to the metal derivatives **2** and **3**. On the other hand, the mobility obtained for the metalated PCs **2** and **3** is higher, which is consistent with the fact that the metallic center plays an important role for the charge conduction inside these organic layers. In the metal PCs, the electrons from nitrogens of neighboring molecules interact with the

metallic center, which thus acts as a bridge between the nitrogen atoms of the stacking molecules, contributing to the enhancement of the π-electron delocalization in comparison to the corresponding metal-free PC. Thus, the higher mobility for Ni and Cu PCs is due to an increased interaction of the molecular orbitals between parallely aligned molecules. Non-mesogenic Ni and Cu PCs exhibit in general a higher mobility than H_2PCs.[41]

4 Conclusions

In summary, regioregularly all-endo tetrasubstituted PCs exhibiting a highly ordered plastic crystalline columnar phase at room temperature give rise to pronounced current rectification in simple ITO/PEDOT:PSS/PC/Al diode structures. These good diode characteristics are obtained despite the preponderantly in-plane alignment of the columns and thus of the axis of preferred charge migration within the PC layer. The field dependent charge carrier mobilities across the devices were obtained in the trap-limited SCLC regimes from the current-voltage curves to be of the order of 10^{-5} cm^2/Vs for the metal-free PC homologue, and of the order of 10^{-4} cm^2/Vs for the metalated Cu and Ni derivatives at +4.6 V. This mobility could still be improved by obtaining a homeotropic alignment of the molecular columns, as previously demonstrated for a perylene based molecule, where an increase of 5 orders of magnitude was obtained.[37] The planar alignment is disadvantageous in diode-type devices since in this way the charges have to be transported perpendicular to the π-stacking direction. On the other hand such orientation is beneficial for thin film transistors. The XRD, excited-state lifetime and optical absorption characterizations suggest that the π–π intermolecular interactions are stronger for metal-free PC **1**, whereas CuPC **2** and NiPC **3** presented better electrical response. This demonstrates that for phtalocyanines the intermolecular ligand-ligand π-π interactions do not dominate the electrical conduction, confirming that the metallic centre plays an important role for the charge transport inside these materials.

Associated Content

Supporting Information

Absorption spectra of H_2PC and CuPC in solution and film, comparison between the mono-exponential fitting for H_2PC in solution and bi-exponential in spin-coated film, fluorescence spectra of **1-3** excited at 636 nm in solution and thin film, AFM analysis of PCs **1** and **2** before annealing and after annealing for **2**, and mobility of the PCs at the SCLC regime as a function of the applied voltage.

Author information

Corresponding Author

E-mail: juh_19@yahoo.com.br

*Phone: +55 48 37212304. Fax: +55 48 37219946.

E-mail: ivan.bechtold@ufsc.br

*Phone: +55 48 37212304. Fax: +55 48 37219946.

Notes

The authors declare no competing financial interest.

Acknowledgements

This research was financed partially by a Coordenação de Aperfeiçoamento de Pessoal de Nível Superior - Comité Français d'Evaluation de la Coopération Universitaire et Scientifique avec le Brésil (CAPES-COFECUB, project Ph-C 803-14) grantand by CNPq, Capes, FAPEMIG and INCT/INEO funds. The XRD experiments were carried out in the Laboratório de Difração de Raios-X (LDRX-CFM/UFSC).

References

1 D. Wohrle, G. Schnurpfeil, S. G. Makarov, A. Kazarin and O. N. Suvorova, *Macroheterocycles*, 2012, **5**, 191-202.

2 F. Yakuphanoglu, M. Kandaz, M. N. Yarasir and F. B. Senkal, *Physica B*, 2007, **393**, 235-238.

3 C. W. Tang, *Appl Phys Lett*, 1986, **48**, 183-185.

4 L. M. Ozer, M. Ozer, A. Altindal, A. R. Ozkaya, B. Salih and O. Bekaroglu, *Dalton T*, 2013, **42**, 6633-6644.

5 E. Ozerden, M. Yildiz, Y. S. Ocak, A. Tombak and T. Kilicoglu, *Mat Sci Semicon Proc*, 2014, **28**, 72-76.

6 N. B. McKeown, *Phthalocyanine materials : synthesis, structure, and function*. (Cambridge University Press, Cambridge, 1998).

7 M. A. Rauf, S. Hisaindee, J. P. Graham and M. Nawaz, *J Mol Liq*, 2012, **168**, 102-109.

8 C. Piechocki, J. Simon, A. Skoulios, D. Guillon and P. Weber, *J Am Chem Soc*, 1982, **104**, 5245-5247.

9 D. Atilla, G. Aslibay, A. G. Gurek, H. Can and V. Ahsen, *Polyhedron*, 2007, **26**, 1061-1069.

10 B. R. Kaafarani, *Chem Mater*, 2011, **23**, 378-396.

11 M. O'Neill and S. M. Kelly, *Adv Mater*, 2011, **23**, 566-584.

12 R. J. Bushby, S. M. Kelly, M. O'Neill and SpringerLink (Online service), *Liquid Crystalline Semiconductors : Materials, properties and applications*.

13 S. Laschat, A. Baro, N. Steinke, F. Giesselmann, C. Hagele, G. Scalia, R. Judele, E. Kapatsina, S. Sauer, A. Schreivogel and M. Tosoni, *Angew Chem Int Edit*, 2007, **46**, 4832-4887.

14 J. Meiss, A. Merten, M. Hein, C. Schuenemann, S. Schafer, M. Tietze, C. Uhrich, M. Pfeiffer, K. Leo and M. Riede, *Adv Funct Mater*, 2012, **22**, 405-414.

15 H. Hayashi, W. Nihashi, T. Umeyama, Y. Matano, S. Seki, Y. Shimizu and H. Imahori, *J Am Chem Soc*, 2011, **133**, 10736-10739.
16 N. B. Chaure, C. Pal, S. Barard, T. Kreouzis, A. K. Ray, A. N. Cammidge, I. Chambrier, M. J. Cook, C. E. Murphy and M. G. Cain, *J Mater Chem*, 2012, **22**, 19179-19189.
17 P. Apostol, A. Bentaleb, M. Rajaoarivelo, R. Clerac and H. Bock, *Dalton T*, 2015, **44**, 5569-5576.
18 D. V. O'Connor and D. Phillips, *Time-correlated single photon counting*. (Academic, London, 1984).
19 L. D. Rollmann and R. T. Iwamoto, *J Am Chem Soc*, 1968, **90**, 1455-&.
20 M. K. Masahiro Hiramoto, Yusuke Shinmura, Norihiro Ishiyama, Toshihiko Kaji, Kazuya Sakai, Toshinobu Ohno, Masanobu Izaki *Electronics*, 2014, **3**.
21 I. H. Bechtold, J. Eccher, G. C. Faria, H. Gallardo, F. Molin, N. R. S. Gobo, K. T. de Oliveira and H. von Seggern, *J Phys Chem B*, 2012, **116**, 13554-13560.
22 L. Y. Yang, M. M. Shi, M. Wang and H. Z. Chen, *Tetrahedron*, 2008, **64**, 5404-5409.
23 S. Hellstrom, F. L. Zhang, O. Inganas and M. R. Andersson, *Dalton T*, 2009, 10032-10039.
24 M. N. Sibata, A. C. Tedesco and J. M. Marchetti, *Eur J Pharm Sci*, 2004, **23**, 131-138.
25 M. Ambroz, A. Beeby, A. J. Macrobert, M. S. C. Simpson, R. K. Svensen and D. Phillips, *J Photoch Photobio B*, 1991, **9**, 87-95.
26 G. Valduga, E. Reddi, G. Jori, R. Cubeddu, P. Taroni and G. Valentini, *J Photoch Photobio B*, 1992, **16**, 331-340.
27 P. Bertoncello and M. Peruffo, *Colloid Surface A*, 2008, **321**, 106-112.
28 I. O. Shklyarevskiy, P. Jonkheijm, N. Stutzmann, D. Wasserberg, H. J. Wondergem, P. C. M. Christianen, A. P. H. J. Schenning, D. M. de Leeuw, Z. Tomovic, J. S. Wu, K. Mullen and J. C. Maan, *J Am Chem Soc*, 2005, **127**, 16233-16237.
29 J. Piris, M. G. Debije, N. Stutzmann, A. M. van de Craats, M. D. Watson, K. Mullen and J. M. Warman, *Adv Mater*, 2003, **15**, 1736-+.
30 E. Charlet, E. Grelet, P. Brettes, H. Bock, H. Saadaoui, L. Cisse, P. Destruel, N. Gherardi and I. Seguy, *Appl Phys Lett*, 2008, **92**.
31 S. Archambeau, I. Seguy, P. Jolinat, J. Farenc, P. Destruel, T. P. Nguyen, H. Bock and E. Grelet, *Appl Surf Sci*, 2006, **253**, 2078-2086.
32 E. Grelet, S. Dardel, H. Bock, M. Goldmann, E. Lacaze and F. Nallet, *Eur Phys J E*, 2010, **31**, 343-349.
33 T. M. Brown and F. Cacialli, *J Polym Sci Pol Phys*, 2003, **41**, 2649-2664.
34 J. Eccher, W. Zajaczkowski, G. C. Faria, H. Bock, H. von Seggern, W. Pisula and I. H. Bechtold, *Acs Appl Mater Inter*, 2015, **7**, 16374-16381.
35 C. H. Kim, H. Hlaing, S. Yang, Y. Bonnassieux, G. Horowitz and I. Kymissis, *Org Electron*, 2014, **15**, 1724-1730.
36 J. M. Mativetsky, H. Wang, S. S. Lee, L. Whittaker-Brooks and Y. L. Loo, *Chem Commun*, 2014, **50**, 5319-5321.
37 J. Eccher, G. C. Faria, H. Bock, H. von Seggern and I. H. Bechtold, *Acs Appl Mater Inter*, 2013, **5**, 11935-11943.
38 J. M. Warman and P. G. Schouten, *J Phys Chem-Us*, 1995, **99**, 17181-17185.
39 M. G. Debije, J. Piris, M. P. de Haas, J. M. Warman, Z. Tomovic, C. D. Simpson, M. D. Watson and K. Mullen, *J Am Chem Soc*, 2004, **126**, 4641-4645.
40 J. Simmerer, B. Glusen, W. Paulus, A. Kettner, P. Schuhmacher, D. Adam, K. H. Etzbach, K. Siemensmeyer, J. H. Wendorff, H. Ringsdorf and D. Haarer, *Adv Mater*, 1996, **8**, 815-&.
41 L. Q. Li, Q. X. Tang, H. X. Li, W. Hu, X. O. Yang, Z. Shuai, Y. Q. Liu and D. Zhu, *Pure Appl Chem*, 2008, **80**, 2231-2240.